Reversible Opening of the Triangular Structure of a Sulfido-bridged ZrRh$_2$ Early-Late Heterobimetallic Complex Induced by Bis-(diphenylphosphino)methane.

Marc A. F. Hernandez-Gruel, Fernando J. Lahoz, Isabel T. Dobrinovich, F. Javier Modrego,

Luis A. Oro* and Jesús J. Pérez-Torrente*

Departamento de Química Inorgánica, Instituto Universitario de Catálisis Homogénea,

Instituto de Ciencia de Materiales de Aragón, Universidad de Zaragoza-C.S.I.C., 50009-

Zaragoza, Spain.

e-mail: oro@unizar.es, perez@unizar.es*;* Fax. 34 976761143.

Abstract

Reaction of the early-late heterobimetallic complexes $[Cp^{tt}_2Zr(\mu_3-S)_2\{M(CO)\}_2(\mu-dppm)]$ (M = Rh, Ir) with dppm (bis-(diphenylphosphino)methane) yields the compounds $[Cp^{tt}_2Zr(\mu-S)_2M(\mu-CO)_2(\mu-dppm)M(\eta^2-dppm)]$ (M = Rh (**3**), Ir (**4**)). The molecular structure of **3** shows a bent trimetallic ZrRhRh chain with tetrahedral, trigonal-bipyramidal and square-piramidal geometries, respectively. This trinuclear compound exhibits a mixed-valence Rh(II)−Rh(0) metal-metal bonded unit that results form the unusual chelating coordination of the metalloligand $[Cp^{tt}_2Zr(S)_2]^{2-}$ and is further stabilized by the presence of two unsymmetrical bridging carbonyl ligands which interact with the unsaturated Rh(II) metal. The formation of **3** is reversible and the equilibrium **1** + dppm $\leftrightarrows$ **3** has been observed in solution (K ≈ 16 at 22 ºC in C_6D_6). The opening of the triangular core in the heterotrimetallic compound $[Cp^{tt}_2Zr(\mu_3-S)_2\{Rh(CO)\}\{Ir(CO)\}(\mu-dppm)]$ (**5**) is not selective and gives the compounds $[Cp^{tt}_2Zr(\mu-S)_2Rh(\mu-CO)_2(\mu-dppm)Ir(\eta^2-dppm)]$ (**6**) and $[Cp^{tt}_2Zr(\mu-S)_2Ir(\mu-CO)_2(\mu-dppm)Rh(\eta^2-dppm)]$ (**7**) in a 3:1 molar ratio.

Introduction

The main interest on early-late heterobimetallic (ELHB) complexes is based on the reasonable expectations of a distinctive reactivity associated with the interplay of widely electronically divergent transition metals.[1] The combination of electron-poor early transition metals and electron-rich late transition metals in a single compound allows the potential for synergistic effects to promote unusual reactivity patterns with applications both in synthesis [2] and catalysis.[3] However, the structural diversity of ELHB complexes and the new bonding schemes, arising from the unique electronic structures originated from the gradient of d orbital energy levels of the two metals, are also aspects of special significance.[4] In addition, the study of the metal-metal interactions in ELHB complexes and their consequences on the reactivity could help to the modelling of the strong metal-support interactions (SMSI) observed in heterogeneous catalysts based on late transition metals on a Lewis acid support.[5]

In this context, we have shown that deprotonation of the bis(hydrosulfido)titanium complex $[Cp_2Ti(SH)_2]$ with standard d^8 rhodium and iridium compounds containing basic ligands is a convenient entry to the synthesis of d^0-d^8 sulfido-bridged ELHB complexes with unusual structures as for example, the heterotetranuclear complexes $[CpTi(\mu_3\text{-}S)_3\{M(diolefin)\}_3]$ with a incomplete cubane structure,[6] the heterotrinuclear complexes $[Cp(acac)Ti(\mu_3\text{-}S)_2\{M(diolefin)\}_2]$ (M = Rh, Ir) with a triangular structure,[7] the oxo-sulfido clusters $[(CpTi)_2(\mu_4\text{-}O)(\mu_2\text{-}S)_4Rh_4(CO)_4(PR_3)_2]$ with an incomplete double-fused cubane structure,[8] or the distorted tetrahedral clusters $[CpTi(\mu_3\text{-}S)_3Ir_3(\mu\text{-}CO)(CO)_3(PR_3)_3]$ that contain a tetrahedral iridium center and exhibit an unusual dynamic behavior involving mobility of metal-metal bonds.[9] In sharp contrast, deprotonation of the bis(hydrosulfido)zirconium complex $[Cp^{tt}_2Zr(SH)_2]$ ($Cp^{tt} = \eta^5\text{-}1,3\text{-}di\text{-}tert\text{-}butylcyclopentadienyl$) gave the expected ELHB heterotrinuclear complexes $[Cp^{tt}_2Zr(\mu_3\text{-}S)_2\{ML_2\}_2]$ with a triangular $[ZrM_2]$ (M = Rh, Ir) core capped with two μ_3-sulfido ligands.[10]

Interestingly, the carbonyl iridium complex $[Cp^{tt}_2Zr(\mu_3\text{-}S)_2\{Ir(CO)_2\}_2]$ is a precursor for the synthesis of early-late heterotrimetallic (ELHT) complexes by metal exchange reactions through the ion-pair compound $[Ir(CO)(dppe)_2][Cp^{tt}_2Zr(\mu\text{-}S)_2Ir(CO)_2]$ that results from the reaction with 1,2-bis(diphenylphosphino)ethane (dppe).[11] Nevertheless, the triangular $[ZrM_2]$ core is preserved in the reactions with other diphosphines and, for example, the complexes $[Cp^{tt}_2Zr(\mu_3\text{-}S)_2\{M(CO)\}_2(\mu\text{-}dppm)]$ (M = Rh, Ir) were cleanly obtained from the reaction of $[Cp^{tt}_2Zr(\mu_3\text{-}S)_2\{M(CO)_2\}_2]$ with bis(diphenylphosphino)methane (dppm). However, we have discovered that this reaction is more complicated than could be anticipated. We report herein a dppm-induced structural rearrangement that results in an unusual equilibrium between trinuclear ELHB complexes.

Results

Reaction of the complexes $[Cp^{tt}_2Zr(\mu_3\text{-}S)_2\{M(CO)_2\}_2]$ (M = Rh, Ir) with dppm. The carbonyl replacement reactions on the complex $[Cp^{tt}_2Zr(\mu_3\text{-}S)_2\{Rh(CO)_2\}_2]$ by P-donor ligands usually take place quickly at room temperature. Although the reaction with monodentate ligands, as for example $P(OR)_3$, can be stopped at the disubstituted $[Cp^{tt}_2Zr(\mu_3\text{-}S)_2\{Rh(CO)(P(OR)_3)\}_2]$ complexes, which were isolated as a *cis/trans* mixture of isomers,[10] these species were found to react further with $P(OR)_3$ with evolution of carbon monoxide. We have observed that the triangular $[ZrRh_2]$ core is also maintained after the replacement of two carbonyl groups by the short-bite bidentate dppm ligand to give the complex $[Cp^{tt}_2Zr(\mu_3\text{-}S)_2\{Rh(CO)\}_2(\mu\text{-}dppm)]$ (**1**), in which the dppm ligand bridges the rhodium atoms with a *cisoid* arrangement.[10] However, in contrast with monodentate P-donor ligands, the compound **1** reacts further with dppm without replacement of additional carbonyl ligands.

The reaction of the complex $[Cp^{tt}_2Zr(\mu_3\text{-S})_2\{Rh(CO)_2\}_2]$ with an excess of dppm in toluene gave a red-brown solution from which the complex $[Cp^{tt}_2Zr(\mu\text{-S})_2Rh(\mu\text{-CO})_2(\mu\text{-dppm})Rh(\eta^2\text{-dppm})]$ (**3**) was isolated as dark-red crystals in moderate yield. The structure has been determined by X-ray diffraction methods (Figure 1) and is discussed below. In order to gain further insight into the formation of compound **3**, the reaction of $[Cp^{tt}_2Zr(\mu_3\text{-S})_2\{Rh(CO)_2\}_2]$ with dppm was monitored by $^{31}P\{^1H\}$ and ^1H NMR spectroscopy. Thus, the reaction with one molar-equiv of dppm in C_6D_6 at RT gave a dark green solution of the complex $[Cp^{tt}_2Zr(\mu_3\text{-S})_2\{Rh(CO)\}_2(\mu\text{-dppm})]$ (**1**) which features a characteristic broad doublet at δ 24.9 ppm ($J_{Rh\text{-}P}$ = 169 Hz) at RT. The reaction of $[Cp^{tt}_2Zr(\mu_3\text{-S})_2\{Rh(CO)_2\}_2]$ with two molar-equiv of dppm under the same conditions (≈ 0.3 M) resulted in the formation of $[Cp^{tt}_2Zr(\mu\text{-S})_2Rh(\mu\text{-CO})_2(\mu\text{-dppm})Rh(\eta^2\text{-dppm})]$ (**3**) which coexist with **1** and dppm (Figure 2). Compound **3** exhibits three characteristic resonances in the $^{31}P\{^1H\}$ NMR spectrum in a 1:1:2 ratio in full agreement with the structure found in the solid state. The product distribution deduced from the integral of the Cp^{tt} resonances in the ^1H NMR spectrum was 45% (**1**) and 55% (**3**). Obviously, the same product distribution was found when **1** was reacted with just one molar-equiv of dppm. In addition, it was observed that further addition of dppm increased the **3** to **1** complex ratio. For example, the product distribution resulting from the reaction of $[Cp^{tt}_2Zr(\mu_3\text{-S})_2\{Rh(CO)_2\}_2]$ with three molar-equiv of dppm was 30% (**1**) and 70% (**3**). These observations strongly suggest that compounds **1** and **3** could be in a dynamic equilibrium mediated by dppm. On the other hand, the dark red crystals of compound **3**, that gave a red powder when crushed, afforded dark green solutions in toluene that are indicative of the presence of compound **1**. In fact, the $^{31}P\{^1H\}$ NMR of the crystals in C_6D_6 showed the presence of **1**, **3** and dppm, which confirm the existence of the equilibrium **1** + dppm ⇆ **3**. The equilibrium constant, determined by the integral of characteristic resonances (Cp^{tt} and $>CH_2$)

of the different species, was found to be roughly 16 at 22 ºC in C_6D_6. As expected, the equilibrium is solvent dependent and is shifted towards compound **1** in more polar solvents as CD_2Cl_2 or $CDCl_3$.

The reaction of $[Cp^{tt}_2Zr(\mu_3-S)_2\{Ir(CO)_2\}_2]$ with two molar-equiv of dppm in toluene, or alternatively the reaction of the intermediate complex $[Cp^{tt}_2Zr(\mu_3-S)_2\{Ir(CO)\}_2(\mu-dppm)]$ (**2**) with one molar-equiv, gave an orange-red solution of complex $[Cp^{tt}_2Zr(\mu-S)_2Ir(\mu-CO)_2(\mu-dppm)Ir(\eta^2-dppm)]$ (**4**) which was isolated as a brick red microcrystalline solid. However, both complexes are not in equilibrium since the conversion of **2** into **4** is complete as evidenced the monitoring of the reaction by $^{31}P\{^1H\}$ NMR. Moreover, compound **4** is not stable in solution and progressively decomposed to give a red-purple solution of the dinuclear complex $[Ir_2(\mu-S)(\mu-dppm)_2(CO)_2]$[12] which exhibited a characteristic singlet resonance at δ -5.0 ppm in the $^{31}P\{^1H\}$ NMR spectrum (d^8-toluene). In fact, the degradation of **4** was completed in 3 hours and compound $[Ir_2(\mu-S)(\mu-dppm)_2(CO)_2]$ could be isolated directly as a purple solid when the reaction was conducted in benzene. The fate of the remaining "Cp^{tt}_2ZrS" fragment was not investigated any further.

Complexes **3** and **4** were characterized by elemental analysis, FAB+ mass spectra and NMR spectroscopy. The spectroscopic data suggest that both complexes are isostructural. The ^1H NMR spectra (C_6D_6) evidenced the presence of a molecular symmetry plane in both molecules in agreement with the approximately C_s symmetry found in the solid state structure for **3** (Figure 1). In fact, although both Cp^{tt} ligands are symmetry related, the protons and ^tBu groups of each cyclopentadienyl ligand are unequivalent and were observed as three triplets between 6.0 and 5.5 ppm and two singlets between 1.85 and 1.33 ppm, respectively. The diastereotopic $>CH_2$ protons of the chelating dppm ligand were observed as two broad multiplets at δ 3.71 and 3.39 ppm for **3** and as a multiplet at δ 4.25 ppm for **4**, whereas the

equivalent >CH_2 protons of the bridging dppm ligand displayed a broad triplet in both compounds. The $^{31}P\{^1H\}$ NMR spectra in C_6D_6 of both compounds (table 1) showed three strongly coupled resonances in a 1:1:2 ratio, in full agreement with the symmetry of the molecules. The observed high field resonance is consistent with the presence of a chelating dppm ligand having equivalent P donor atoms.[13] On the other hand, the measured coupling constants are in accordance with the *cisoid* disposition of the bridging and chelating dppm ligands coordinated to the same metallic center, and are in agreement with those found in the complex [CpFe(μ-CO)(μ-dppm)Rh(η^2-dppm)] with a similar structural disposition of both dppm ligands.[14] In particular, the largest Rh-P and P-P coupling constants correspond to P_B, which exhibit a J_{Rh-P} of 154 Hz and a residual coupling (5 Hz) with the second rhodium atom in **3**, and P_A-P_B couplings of 175 Hz (**3**) and 135 Hz (**4**). The equivalent bridging carbonyl ligands of **3** were observed as a complex symmetric multiplet at δ 230.4 in the $^{13}C\{^1H\}$ NMR spectrum in C_6D_6. In addition, they were observed in the IR spectra as a strong ν(CO) absorption at 1776 (**3**) and 1727 cm^{-1} (**4**), with a weak shoulder at a higher frequency. These relatively low frequency values are comparable to those observed in structurally related carbonyl-bridged dirhodium complexes and could be associated with a stronger back-bonding from the metals.[15]

The reaction of the ELHT complex [$Cp^{tt}_2Zr(\mu_3$-S$)_2${Rh(CO$)_2$}{Ir(CO$)_2$}] with dppm was also investigated for comparative purposes. Thus, the reaction with one-molar equiv of dppm in dichloromethane cleanly afforded the compound [$Cp^{tt}_2Zr(\mu_3$-S$)_2${Rh(CO)}{Ir(CO)}(μ-dppm)] (**5**) which was isolated as a black-greenish microcrystalline solid in good yield. The compound displayed the molecular ion in the FAB+ mass spectrum at m/z 1244 and showed two strong ν(CO) absorptions in the IR at 1957 and 1940 cm^{-1}. The spectroscopic data are in full agreement with a bridging coordination mode of the dppm ligand. Thus, the $^{31}P\{^1H\}$

NMR spectra in CDCl$_3$ showed the expected two resonances at δ 29.60 (dd, J$_{Rh-P}$ = 168 Hz, J$_{P-P}$ = 34 Hz) and 13.73 (d, J$_{P-P}$ = 34 Hz) ppm for the P atoms bonded to the rhodium and iridium atoms, respectively. In addition, the ^{1}H NMR is in accordance the lack of symmetry of the molecule. Treatment of [Cp$^{tt}_2$Zr(μ$_3$-S)$_2${Rh(CO)$_2$}{Ir(CO)$_2$}] with two-molar equiv of dppm or, alternatively, the reaction of **5** with only one-molar equiv (C$_6$D$_6$) gave the complexes [Cp$^{tt}_2$Zr(μ-S)$_2$Rh(μ-CO)$_2$(μ-dppm)Ir(η^2-dppm)] (**6**) and [Cp$^{tt}_2$Zr(μ-S)$_2$Ir(μ-CO)$_2$(μ-dppm)Rh(η^2-dppm)] (**7**) in a 3:1 molar ratio. As can be deduced from the ^{31}P{^{1}H} NMR data (table 1), the chemical shifts and coupling constants of both compounds compare well with those observed for complexes **3** and **4** and, therefore, they should be isostructural. Thus, the opening of the triangular structure in the heterotrimetallic complexes is unselective and suggests that both d^8 metal centers, rhodium and iridium, are well accommodated in the two different pentacoordinated coordination sites of the structure.

Molecular structure of [Cp$^{tt}_2$Zr(μ-S)$_2$Rh(μ-CO)$_2$(μ-dppm)Rh(η^2-dppm)] (3). The molecular structure of the trinuclear complex **3** is shown in Figure 1. Selected bond distances and angles are collected in Table 2. The structure consists of a bent trimetallic chain with a Zr-Rh-Rh angle of 141.65(2)°. The structure exhibits a dirhodium unit "Rh$_2$(μ-CO)$_2$(μ-dppm)" having two carbonyl and one dppm bridging ligands. If metal-metal bonding interactions are neglected, both rhodium atoms are five-coordinated being bonded to two additional ligands. The geometry around the central rhodium, Rh(1), is that of a trigonal-bipyramid by additional coordination to both sulfur atoms of the metalloligand [Cp$^{tt}_2$Zr(S)$_2$]^2; the axial positions are occupied by P(1) and S(2) donor atoms (174.07(6)°). While the two Zr-S bond distances are very similar, 2.4329 and 2.4245(18) Å, the bipyramidal geometry around Rh(1) and the structural *trans* effect of the phosphine (P(1) atom) make the two Rh(1)-S bond lengths to be significantly different (2.3099(17) *vs* 2.4097(18) Å). In contrast to the described Rh(1) environment, the geometry of the external rhodium atom is square-pyramidal by coordination

to a second quelate η^2-dppm ligand, with the apical position occupied by the P donor atom of the bridging dppm ligand (P(2)). The Zr atom exhibits a distorted pseudo-tetrahedral geometry linked to two η^5-Cp^{tt} ligands and two bridging sulfur atoms. The wide angle centered on the Zr with the two centroids of the Cp^{tt} ligands, 124.93(11)^o, is largely determined by the steric effects of the bulky *tert*-butyl substituents. According with this, both Cp^{tt} ligands adopt a nearly staggered conformation (torsion angle between the Cp^{tt} rings: C(2)-G(1)-G(2)-C(15) 25.5 ^{o}, or C(4)-G(1)-G(2)-G(17) 25.2(5) ^{o}), far from the eclipsed or straddle disposition found in the mononuclear complexes [Cp$^{tt}_2$TiCl$_2$][16] and [Cp$^{tt}_2$ZrI$_2$],[17] respectively. The angle between the idealized planes of both Cp^{tt} ligands of 63.8(3) ^{o} is comparable to that found in the complex **1** (62.1(2)^o)[10] and is enough to allow the free rotation of the Cp^{tt} ligands as was evidenced in the ^{1}H NMR spectrum.

The ligand distribution in the dirhodium metal core results in 15 e$^-$ (trigonal-bipyramidal) and 17 e$^-$ (square-pyramidal) metal centers and, in consequence, a covalent metal-metal bond between both rhodium atoms is expected to be present. In fact, the intermetallic separation between the rhodium atoms, 2.7611(7)Å, lies in the expected range for Rh-Rh single bonds and is comparable to that found in structurally related metal-metal bonded dirhodium dimers [Rh$_2$(CO)$_3$(PPh$_3$)$_3$(μ-CO)$_2$][18] (2.769 Å) and [{Rh(CO)(dppp)}$_2$(μ-CO)$_2$][19] (2.725 and 2.709 (1) Å). Surprisingly, the intermetallic separation is similar to that found in compound **1** (2.7404(6) Å), although in this case the structural and electronic parameters suggest the absence of an attractive intermetallic interaction and point towards the bridging diphosphine ligand as the cause for the short Rh⋯Rh separation observed. On the other hand, the Zr-Rh intermetallic separation of 3.2772(8) Å is shorter than that found in compound **1** (3.3378(11) Å), but excludes any kind of interaction between the metal centers. The short metal-metal distance in the planar "Rh$_2$(μ-CO)$_2$" unit results in small Rh-C-Rh angles, 86.4 and 85.9(3)^o, typical values for carbonyl ligands bridging metal-metal bonded centers.[20] Both carbonyl

bridges display some degree of asymmetry as they slightly point out towards the central trigonal-bipyramidal rhodium atom. The shorter Rh-C bond distances (1.993 and 1.989(7) Å) correspond to the external rhodium atom, Rh(2), and are associated with larger Rh-C-O bond angles of 144.5 and 144.7(5)°. The longer Rh-C bond distances (2.040 and 2.062(7) Å) are with the central rhodium atom, Rh(1), and are associated with smaller Rh-C-O angles (129.0 and 129.4(5)°). This relationship between Rh-C distances and Rh-C-O angles is in agreement with the structural parameters observed for other unsymmetrical bridging carbonyl ligands.[21]

Discussion

The dppm-induced equilibrium between compounds **1** and **3** involves a significant reorganization of ligands between the two late metal centers that also concerns a number of important bonding considerations. From a structural point of view, the formation of complex **3** results from the opening of the compact triangular [ZrRh$_2$] core capped by two μ_3-sulfido in **1** upon coordination of an additional dppm ligand. Assuming that the bridging dppm ligand in **1** is preserved, the introduction of a chelating dppm ligand on one of the rhodium atoms formally causes the shift of the metalloligand [Cp$^{tt}_2$Zr(S)$_2$]$^{2-}$ to the second rhodium center, a change in the coordination mode of both carbonyl ligands that move from terminal to bridging positions, and the formation of a Rh-Rh bond. The [Cp$^{tt}_2$Zr(S)$_2$]$^{2-}$ fragment in **1** is coordinated as μ-(1:2κ^2S;1:2κ^2S') to both rhodium atoms acting as a 6 e$^-$ donor. However, in complex **3** the metalloligand acts as 2 e$^-$ donor as a consequence of the κ^2S,S' coordination to only one of the rhodium centers. As the entering dppm ligand is a 4 e$^-$ donor, the total number of valence electrons in the dirhodium unit remains unchanged (32 e$^-$) upon the formation of **3**. On the other hand, the dirhodium unit in compound **1** consist of two 16 electron Rh(I) centers with the expected square-planar coordinations. However, the metal-metal bonded dirhodium fragment in **3** can be described as a mixed-valence Rh(II)−Rh(0) with 16 and 18 electron

10

configurations, respectively. Thus, the facile interconversion between **1** and **3** could be interpreted as an intramolecular disproportionation of Rh(I)···Rh(I) to Rh(II)−Rh(0) that is easily accommodated by the interplay between the zirconium metalloligand and the dppm ligand.

The presence of unsymmetric bridging carbonyl ligands in **3** further support the existence of a mixed-valence $Rh_2^{II,0}$ central core. Although unsymmetrical bridging of Rh-Rh bonds by carbonyl ligands has been ascribed to steric effects, the electronic effects also play an important role in the case of polar metal-metal bonds.[22] Thus, the structure of **3** features as the C-O vectors bend towards the unsaturated central Rh(II) atom that displays an effective electronic deficit. The metal-metal bonded $M_2^{II,0}$ mixed-valence complexes (M = Rh, Ir) are unusual. Related precedent in the iridium chemistry are the 32 valence electrons complexes $[Cp^*(PMe_3)Ir(\mu\text{-}S)Ir(NO)(PPh_3)]$,[23] that possess a $Ir_2^{II,0}$ dimetal core with 18 and 16 e$^-$ configurations respectively, and $[Cl_2Ir(\mu\text{-tfepma})_2Ir(\eta^2\text{-tfepma})]$[24] [tfepma = $MeN\{P(OCH_2CF_3)_2\}_2$], containing a $Ir_2^{II,0}$ dimetal core with 16 and 18 e$^-$ configuration respectively. It is noticeable that both complexes contain an unsaturated metal center with a 16 e$^-$ configuration as it has been found in compound **3**. On the other hand, the $Rh_2^{II,0}$ dimetal core of the 34 valence electron complex $[Br_2Rh(\mu\text{-dfpma})_3Rh(PPh_3)]$ (dfpma = bis-(difluorophosphino)methylamine) is composed of two saturated rhodium atoms with 18 e$^-$ configuration.[25]

This electronic interplay can be assessed by a series of theoretical studies on model compounds $[Cp_2Zr(\mu_3\text{-}S)_2\{Rh(CO)\}_2(\mu\text{-}(CH_2(PH_2)_2))]$ (**1m**, model of compound **1**) and $[Cp_2Zr(\mu\text{-}S)_2Rh(\mu\text{-}CO)_2(\mu\text{-}(CH_2(PH_2)_2))Rh(\eta^2\text{-}(CH_2(PH_2)_2))]$ (**3m**, model of compound **3**). Calculations have been carried out by full geometrical optimization at DFT level using the b3pw91 functional without symmetry restrictions.

The main structural features are well reproduced in both cases. For compound **1m** the calculated geometrical parameters of the trimetallic core are in agreement with those observed. The Zr-Rh calculated distance is 3.31 Å (3.3170(8) and 3.3428(7) A) and the Rh-Rh separation 2.79 A (2.7404(6) A).[10a] The internal parameters of the trimetallic core of **3** are also well reproduced in **3m**. The calculated Zr-Rh distance is 3.22 Å (3.2772(8) Å) and the Rh-Rh distance is 2.77 Å (2.7611(7)Å) whereas the Zr-Rh-Rh angle of 138º compares well to the observed 141.65(2)º. The asymmetry in the carbonyl ligand bridges is also recovered in the theoretical calculations and supports an electronic origin for this effect. The calculated distances of the central rhodium atom to the carbon bridges are 2.00 and 2.03 Å (2.040 and 2.062(7) Å) and those of the external rhodium atom are 2.01 and 2.02 (1.993 and 1.989(7) Å). The calculated Rh-C-O bond angles to the central rhodium atom are 131.4º and 131.7º (*vs.* 129.0º and 129.4(5)º) and to the external rhodium atom 141.0º and 140.7º (*vs.* 144.5º and 144.7(5)º). It is worth to emphasise that the calculated values properly compare well not only with the absolute values determined in the X-ray experiment, but they also reproduce their relative relationships and trends.

The proposed assignment of oxidation state changes during the reaction is supported by the NBO atomic charges derived from the calculations. NBO charges are 1.00 for Zr and -0.13 for both Rh atoms in compound **1m**. They change to 0.94 for Zr , +0.11 for central Rh atom and -0.16 for the external Rh atom in compound **3m**. The largest change is observed for the central Rh atom that looses a significant amount of electronic density whereas the external Rh experiments a slight increase. Though a direct relationship between formal oxidation state and calculated charges is unrealistic, the model of an oxidation of the central atom and a reduction of the external one in the formation of **3** seems to be supported by this theoretical approach.

NBO analysis of the electronic environment of the bridging carbonyl in **3m** ligands rule out a ketonic character. The Wiberg bond indexes for the C-O bonds change very slightly from

1m (2.09) to **3m** (1.96 and 1.99). This is reflected also in the calculated CO distances (1.16 Å in **1m** and 1.17 Å for both CO bridging ligands in **3m**). On the other hand, the overall NBO charges on the carbonyl ligands are slightly positive in the terminal carbonyl ligands of **1m**, whereas in the bridging carbonyl ligands in **3m** become slightly negatives as a consequence of a lesser positive charge on the carbon atoms since the negative charge on the oxygen atoms remains almost constant. This could reflect a better $\int$ donor role of the terminal carbonyls and a similar acceptor capability of both terminal (**1m**) and bridging (**3m**) carbonyls ligands. The calculated Wiberg bond indexes for the Rh-C bonds of the terminal carbonyl ligands in **1m** are close to 1 (0.94). However, the mean Wiberg indexes for the bridging ligands in **3m** are 0.55 and reflect a weaker Rh-CO interaction, the sum of Wiberg indexes for a given carbonyl with the two rhodium atoms its bridges it is close to 1 (mean 1.1) as the bonding capability is distributed across the bridge.[26] The increase in the metal-metal bond character in **3m** compared to **1m** is observed in the Wiberg index that change from 0.05 in **1m** to 0.13 in **3m**.[27]

As far as the mechanism of formation of the complexes [$Cp^{tt}_2Zr(\mu-S)_2M(\mu-CO)_2(\mu-dppm)M(\eta^2-dppm)$] is concerned, it is worth to mention that the key factor responsible for the opening of the heterotrinuclear structure in the complexes [$Cp^{tt}_2Zr(\mu_3-S)_2\{M(CO)\}_2(\mu-dppm)$] is the breaking of two Rh-S bonds instead of the possible further CO replacement after interaction with dppm. This process, which results in the disconnection of a rhodium center from the metalloligand, is further assisted by chelating coordination of the incoming dppm ligand and the concerted motion both of the zirconium metalloligand to the second rhodium center, and of the terminal carbonyl ligands to the bridging positions. Thus, the crucial factor for this process seems to be the switch of the coordination mode of the zirconium metalloligand [$Cp^{tt}_2ZrS_2$]$^{2-}$ which in turn is able to stabilize the resulting mixed-valence $Rh_2^{II,0}$ dimetal core. Moreover, the overall process is largely facilitated by the short metal-metal

distances in the precursor complexes (2.74 Å in **1**) and for the presence of a bridging dppm ligand that acts as a template for the concerted movement of the carbonyl ligands and the zirconium metalloligand.

The equilibrium **1** + dppm ⇆ **3** represents an uncommon case of reversible metal-metal bond formation. Although the dynamic behavior associated with the presence of mobile metal-metal bonds has few precedents, it has been observed both in clusters[28] and polynuclear complexes.[29] Nevertheless, in the present case the metal-metal bond formation is rather associated to the ligand dynamics,[30] i.e. the reversible dppm-induced change of the coordination mode of the zirconium metalloligand that is the responsible of the change of the electron count on the d^8 metal centers. The formation of the compound $[Cp^{tt}_2Zr(\mu-S)_2Ir(\mu-CO)_2(\mu-dppm)Ir(\eta^2-dppm)]$ (**4**) is irreversible and contrast with the equilibrium observed in the zirconium-rhodium complexes. However, compound **4** is unstable and quantitatively evolves to the dinuclear compound $[Ir_2(\mu-S)(\mu-dppm)_2(CO)_2]$ which results from the degradation of the metalloligand $[Cp^{tt}_2ZrS_2]^{2-}$ via the transfer of a sulfido ligand to the dinuclear iridium fragment.

It is noticeable that a similar core transformation has been observed in the reaction of $[Cp^{tt}_2Zr(\mu_3-S)_2\{Rh(CO)\}_2(\mu-dppm)]$ (**1**) with a different chelating diphosphine. The monitoring of the reaction of **1** with 1,2-bis(diphenylphosphino)ethane (dppe) by $^{31}P\{^1H\}$ NMR showed the formation of the compound $[Cp^{tt}_2Zr(\mu-S)_2Rh(\mu-CO)_2(\mu-dppm)Rh(\eta^2-dppe)]$,[31] that contains bridging μ-dppm and chelating η^2-dppe ligands, and the cation $[Rh(dppe)_2]^+$ (δ 58.23 ppm, J_{Rh-P} = 133 Hz)[32] as the main species. However, the mixed-diphosphine complex quickly evolves to $[Rh(dppe)_2]^+$ as the major dppe-containing species.

The above described result strongly suggests that heterotrinuclear complexes with a bent structure could serve as a models for the key intermediate species involved in the selective

sequestering of an iridium metal center in the compound $[Cp^{tt}_2Zr(\mu_3\text{-}S)_2\{Ir(CO)_2\}_2]$ by dppe to give $[Ir(CO)(dppe)_2][Cp^{tt}_2Zr(\mu\text{-}S)_2Ir(CO)_2]$.[11] This sequestering process is strongly dependent of the diphosphine and seems to be restricted to dppe as no similar process has been observed with dppm. Thus, the potential dppm-induced sequestering process should result in the formation of the heterodinuclear anion $[Cp^{tt}_2Zr(\mu\text{-}S)_2Rh(CO)_2]^-$ and the cation $[Rh(CO)(dppm)_2]^+$ and should be facilitated by the presence of an unsaturated Rh(II) metal center. However, compound **3** did not react further with carbon monoxide in 30 min although extensive decomposition to unidentified species was observed when an equilibrium mixture containing **3** was stirred under a carbon monoxide atmosphere for longer time. In any case, it is noticeable that neither the formation of the cation $[Rh(CO)(dppm)_2]^{+}$ [33] nor $[Rh_2(\mu\text{-}S)(\mu\text{-}dppm)_2(CO)_2]$ [34] were observed.

Concluding Remarks

The opening of the μ_3-sulfido capped triangular core [ZrM$_2$] of the early-late heterobimetallic complexes $[Cp^{tt}_2Zr(\mu_3\text{-}S)_2\{M(CO)\}_2(\mu\text{-}dppm)]$ (M = Rh, Ir) by dppm results in the formation of bent trinuclear complexes $[Cp^{tt}_2Zr(\mu\text{-}S)_2M(\mu\text{-}CO)_2(\mu\text{-}dppm)M(\eta^2\text{-}dppm)]$. These compounds contain a metal-metal bonded M(II)-M(0) subunit resulting from an intramolecular disproportionation process driven by the redistribution of the ligands that takes place after introduction of a new dppm ligand. The stabilization of the mixed-valence dimetal core is attained by the interplay both of the zirconium metalloligand ($Cp^{tt}_2ZrS_2^{2-}$) and the unsymmetrical bridging carbonyl groups which interact with the unsaturated central M(II) metal center. In spite of the significant structural reorganization leading to the new complexes, the formation of the bent [ZrRh$_2$] compound is reversible indicating the existence of a small energy difference between both structures.

Experimental Section

General Methods. All manipulations were performed under a dry argon atmosphere using Schlenk-tube techniques. Solvents were dried by standard methods and distilled under argon immediately prior to use. The complexes $[Cp^{tt}_2Zr(\mu_3\text{-}S)_2\{M(CO)_2\}_2]$, $[Cp^{tt}_2Zr(\mu_3\text{-}S)_2\{M(CO)\}_2(\mu\text{-dppm})]$ (M = Rh, Ir) and $[Cp^{tt}_2Zr(\mu_3\text{-}S)_2\{Rh(CO)_2\}\{Ir(CO)_2\}]$ were prepared as described previously.[10a, 11]

Physical Measurements. ^1H, $^{31}P\{^1H\}$ and $^{13}C\{^1H\}$ NMR spectra were recorded on a Varian Gemini 300 spectrometer operating at 300.08, 121.47 MHz and 75.46 MHz respectively. Chemical shifts are reported in parts per million and referenced to $SiMe_4$ using the residual resonances of the deuterated solvents (^1H and ^{13}C) and 85% H_3PO_4 (^{31}P) as external reference, respectively. IR spectra were recorded on a Nicolet-IR 550 spectrometer. Elemental C, H and N analysis were performed in a 240-C Perkin-Elmer microanalyzer. Mass spectra were recorded in a VG Autospec double-focusing mass spectrometer operating in the FAB$^+$ mode. Ions were produced with the standard Cs$^+$ gun at ca. 30 Kv, 3-nitrobenzylic alcohol (NBA) was used as matrix.

Synthesis of the complexes. $[Cp^{tt}_2Zr(\mu\text{-}S)_2Rh(\mu\text{-}CO)_2(\mu\text{-dppm})Rh(\eta^2\text{-dppm})]$ (3). To a suspension of $[Cp^{tt}_2Zr(\mu\text{-}S)_2\{Rh(CO)_2\}_2]$ (0.040 g, 0.048 mmol) in toluene (5 mL) solid dppm (0.074 g, 0.193 mmol) was added to give a red-brown solution. Slow diffusion of n-hexane into the solution at 258 K gave the complex as dark-red blocks which were collected by filtration, washed with cold n-hexane and then vacuum dried. Yield: 0.034 g (40%). Anal. Calcd for $C_{78}H_{86}O_2P_4S_2Rh_2Zr \cdot 2.5(C_7H_8)$: C, 64.85; H, 6.04; S, 3.62. Found: C, 64.56; H, 6.10; S, 3.38. MS (FAB$^+$, C_6D_6, m/z): 1482 (M$^+$ - 2CO, 11%), 1305 (M$^+$ - 2CO - Cp^{tt}, 100%). ^1H NMR (C_6D_6, 293 K): δ 8.40-6.40 (set of m, 40H, dppm), 5.95, 5.72 and 5.61 (t, $J_{H\text{-}H}$ = 2.6 Hz, 2H each, H_2, H_4 and H_5, Cp^{tt}), 3.71 and 3.39 (br m, 1H each, >CH$_2$, η^2-dppm), 2.32 (br t, $J_{H\text{-}P}$ =

9 Hz, 2H, >CH$_2$, μ-dppm), 1.87 and 1.34 (s, 18H each, CH$_3$, *t*-Bu). ^{13}C{^{1}H} NMR (C$_6$D$_6$, 293 K, selected resonances): δ 230.4 (m, *C*O), 141.7 and 140.5 (C$_1$ and C$_3$), 105.7, 102.1 and 101.9 (C$_2$, C$_4$ and C$_5$), 34.0 and 33.6 (br s, *C*Me$_3$), 32.8 and 32.0 (s, CH$_3$) (Cp^{tt}). IR (CH$_2$Cl$_2$, cm^{-1}): ν(CO), 1817 (w), 1776 (s).

[Cp$^{tt}_2$Zr(μ-S)$_2$Ir(μ-CO)$_2$(μ-dppm)Ir(η^2-dppm)] (4). To a suspension of [Cp$^{tt}_2$Zr(μ-S)$_2$\{Ir(CO)$_2$\}$_2$] (0.060 g, 0.060 mmol) in toluene (2 mL) solid dppm (0.057 g, 0.150 mmol) was added to give an orange solution in 5 min. The solution was concentrated under vacuum (1 mL) and then n-hexane (10 mL) was added. Concentration of the resulting suspension under vacuum to ca. 4 mL gave the compound as a microcrystalline brick red solid which was isolated by filtration, washed with cold n-hexane and dried under vacuum. Yield: 0.082 g (80%). Anal. Calcd for C$_{78}$H$_{86}$O$_2$P$_4$S$_2$Ir$_2$Zr: C, 54.49; H, 5.04; S, 3.73. Found C, 54.20; H, 4.75; S, 3.53. MS (FAB$^+$, CDCl$_3$, m/z): 1718 (M$^+$, 3%), 1690 (M$^+$ - CO, 8%), 1484 (M$^+$ - 2CO - Cp^{tt}, 73%), 1333 (M$^+$ - dppm, 16%), 1157 (M$^+$ - Cp^{tt} - dppm, 47%). ^{1}H NMR (C$_6$D$_6$, 293 K): δ 7.84-6.53 (set of m, 40H, dppm), 5.97, 5.71 and 5.59 (t, J$_{H-H}$ = 2.7 Hz, 2H each, H$_2$, H$_4$ and H$_5$, Cp^{tt}), 4.25 (br m, 2H, >CH$_2$, η^2-dppm), 1.82 (br t, J$_{H-P}$ = 9 Hz, 2H, >CH$_2$, μ-dppm), 1.83 and 1.33 (s, 18H each, *t*-Bu). IR (CH$_2$Cl$_2$, cm^{-1}): ν(CO), 1774 (w), 1727 (s).

[Cp$^{tt}_2$Zr(μ_3-S)$_2$\{Rh(CO)\}\{Ir(CO)\}(μ-dppm)] (5). A solid mixture of [Cp$^{tt}_2$Zr(μ_3-S)$_2$\{Rh(CO)$_2$\}\{Ir(CO)$_2$\}] (0.060 g, 0.065 mmol) and dppm (0.025 g, 0.065 mmol) was dissolved in dichloromethane (5 mL) to give a dark brown-orange solution after evolution of carbon monoxide. The solution was stirred for 10 min and then concentrated under vacuum (1 mL). The slow addition of n-hexane (10 mL) gave a dark suspension that was concentrated under vacuum (3 mL) and cooled at 258 K. The black-greenish microcrystalline solid was isolated by filtration, washed with cold n-hexane and dried under vacuum. Yield: 0.062 g (76%). Anal. Calcd for C$_{53}$H$_{64}$O$_2$P$_2$S$_2$IrRhZr: C, 51.11; H, 5.18; S, 5.15. Found C, 51.18; H,

5.10; S, 5.08. MS (FAB$^+$, CDCl$_3$, m/z): 1244 (M$^+$, 25%), 1188 (M$^+$ - CO, 100%), 1039 (M$^+$ - CO - Cp^{tt}, 70%). ^{1}H NMR (CDCl$_3$, 293 K): 7.65-6.95 (set of m, 20H, dppm), 5.93 (br, 1H), 5.72 (br, 3H), 5.58 (br, 1H), 5.12 (br, 1H) (H$_2$, H$_4$ and H$_5$, Cp^{tt}), 3.66 and 3.49 (br m, 1H each, >CH$_2$), 1.40, 1.30, 1.08 and 0.92 (s, 9H each, *t*-Bu). ^{31}P{^{1}H} NMR (CDCl$_3$, 293 K): δ 29.60 (dd, J$_{Rh-P}$ = 168 Hz, J$_{P-P}$ = 34 Hz), 13.73 (d, J$_{P-P}$ = 34 Hz). IR (CH$_2$Cl$_2$, cm^{-1}): ν(CO), 1957 (s), 1940 (s).

Crystal Structure Determination of [Cp$^{tt}_2$Zr(μ-S)$_2$Rh(μ-CO)$_2$(μ-dppm)Rh(η^2-dppm)] (3). A summary of crystal data, data collection and refinement parameters are given in Table 3. Intensity data were collected for **3** at low temperature (173(2) K) on a CCD Bruker SMART APEX diffractometer with graphite-monochromated Mo-K$_\alpha$ radiation (λ = 0.71073 Å) by using ω rotations (0.3°). Instrument and crystal stability were evaluated by measuring equivalent reflections at different times; no significant decay was observed. Data were corrected for Lorentz and polarization effects, and a semiempirical absorption correction was applied.[35] The structure was solved by Patterson and difference Fourier methods.[36] All non-hydrogen atoms of the metal complex were refined with isotropic and subsequent anisotropic displacement parameters. At this stage of refinement, four spatial regions showed the presence of several disordered toluene molecules. A model for solvent disorder was established completing 2.5 toluene molecules; occupancy factors were fixed from the observation of thermal parameters. In some cases, some geometrical restrains were necessary to properly refine these solvent atoms. Due to the heavy disorder observed in one case, the corresponding methyl group was not included in this molecule. Hydrogen atoms for the trinuclear metal complex were included in calculated positions and refined with positional and displacement riding parameters. Refinements were carried out by full-matrix least-squares on

F^2 (SHELXL-97).[36] The highest residuals (max. 1.07 e/Å^3) were found in close proximity of the disordered atoms; they have no chemical sense.

Theoretical calculations. All computations were performed using the Gaussian 03 package.[37] The structures of the model compounds, **1m** and **3m**, were fully optimized without geometrical constraint using the b3pw91 functional. The basis sets used were: 6-31G** for C,P and S, 6-31G for H and the LANL2DZ basis sets and its associated effective core potentials for the metal atoms. The electronic densities were calculated by the NBO routines.[38]

Supporting Information Available: An X-ray crystallographic file in CIF format for the structure determination of compound **3**. This material is available free of charge via Internet at http://pubs.acs.org.

References

1.- (a) Wheatley, N.; Kalck, P. *Chem. Rev.* **1999**, *99*, 3379. (b) Casey, C. P. *J. Organomet. Chem.* 1990, *400*, 205. (c) Stephan, D. W. *Coord. Chem. Rev.* **1989**, *95*, 41.

2.- (a) Arashiba, K.; Matsukawa, S.; Kuwata, S.; Tanabe, Y.; Iwasaki, M.; Ishii, Y. *Organometallics* **2006**, *25*, 560. (b) Cornelissen, C.; Erker, G.; Kehr, G.; Fröhlich, R. *Organometallics* **2005**, *24*, 214. (c) Corneliβen, C.; Erker, G.; Kehr, G.; Fröhlich, R. *Dalton*

Trans. **2004**, 4059. (d) Takeuchi, D.; Kuwabara, J.; Osakada, K. *Organometallics* **2003**, *22*, 2305. (e) Kato, H.; Seino, H.; Mizobe, Y.; Hidai, M. *J. Chem. Soc. Dalton Trans*. **2002**, 1494. (f) Ikada, T.; Mizobe, Y.; Hidai, M. *Organometallics* **2001**, *20*, 4441. (g) Lutz, M.; Haukka, M.; Pakkanen, T. A.; Gade, L. H. *Organometallics* **2001**, *20*, 2631. (h) Fulton, J. R.; Hanna, T. A.; Bergman, R. G. *Organometallics* **2000**, *19*, 602, (i) Gade, L. H.; Memmler, H.; Kauper, U.; Schneider, A.; Fabre, S.; Bezougli, I.; Lutz, M.; Galka, C.; Scowen, I. J.; McPartlin. M. *Chem. Eur. J.* **2000**, *6*, 692. (j) Aubart, M. A.; Bergman, R. G. *J. Am. Chem. Soc.* **1996**, *118*, 1793. (k) Hanna, T.; Baranger, A. M.; Bergman, R. G. *Angew. Chem. Int. Ed*. **1996**, *35*, 653. (l) Baranger, A. M.; Hanna, T. A.; Bergman, R. G. *J. Am. Chem. Soc.* **1995**, *117*, 10041. (m) Hanna, T. A.; Baranger, A. M.; Bergman, R. G. *J. Am. Chem. Soc.* **1995**, *117*, 11363.

3.- (a) Kuwabara, J.; Takeuchi, D.; Osakada, K. *Chem. Commun*. **2006**, 3815. (b) Comte, V.; Le Gendre, P.; Richard, P.; Moïse, C. *Organometallics* **2005**, *24*, 1439. (c) Goux, J.; Le Gendre, P.; Richard, P.; Moïse, C. *J. Organomet. Chem.* **2005**, *690*, 301. (d) Takayama, C.; Yamaguchi, Y.; Mise, T.; Suzuki, N. *J. Chem. Soc., Dalton Trans*. **2001**, 948. (e) Takayama, C.; Yamaguchi, Y.; Mise, T.; Suzuki, N. *J. Chem. Soc. Dalton Trans*. **2001**, 948. (f) Bosch, B. E.; Brümmer, I.; Kunz, K.; Erker, G.; Fröhlich, R.; Kotila, S. *Organometallics* **2000**, *19*, 1255. (g) Yamaguchi, Y.; Suzuki, N.; Mise, T.; Wakatsuki, Y. *Organometallics* **1999**, *18*, 996. (h) Dickson, R. S.; Bowen, J.; Campi, E. M.; Jackson, W. R.; Jonasson, C. A. M.; McGrath, F. J.; Paslow, D. J.; Polas, A.; Renton, P.; Gladiali, S. *J. Mol. Cat. A-Chem*. **1999**, *150*, 133. (i) Trzeciak, A. M.; Ziólkowski, K. J.; Choukroun, R. *J. Mol. Cat. A-Chem*. **1996**, *110*, 135. (j) Hostetler, M. J.; Butts, M. D.; Bergman, R. G. *J. Am. Chem. Soc.* **1993**, *115*, 2743. (k) Kalck, P.; Serra, C.; Machet, C.; Broussier, R.; Gautheron, B.; Delmas, G.; Trouve, G.; Kubicki, M. *Organometallics* **1993**, *12*, 1021. (l) Hostetler, M. J.; Bergman, R. G. *J. Am. Chem. Soc.* **1990**, *112*, 8621.

4.- (a) Bareille, L.; Le Gendre, P.; Richard, P.; Moïse, C. *Eur. J. Inorg. Chem.* **2005**, 2451. (b) Mokuolu, Q. F.; Duckmanton, P. A.; Hitchcock, P. B.; Wilson, C.; Blake, A. J.; Shukla, L.; Love, J. B. *Dalton Trans.* **2004**, 1960. (c) Takei, I.; Suzuki, K,; Enta, Y.; Dohki, K.; Suzuki, T.; Mizobe, Y. Hidai, M. *Organometallics* **2003**, *22*, 1790. (d) Kuwata, S.; Nagano, T.; Matsubayashi, A.; Ischii, Y.; Hidai, M. *Inorg. Chem.* **2002**, *41*, 4324. (e) Freitag, K.; Gracia, J.; Martín, A.; Mena, M.; Poblet, J.-M.; Sarasa, J. P.; Yélamos, C. *Chem. Eur. J.* **2001**, 07, 3645. (f) Hidai, M.; Kuwata, S.; Mizobe, Y. *Acc. Chem. Res.* **2000**, *33*, 46. (g) Nagano, T.; Kuwata, S.; Ischii, Y.; Hidai, M. *Organometallics* **2000**, *19*, 4176.

5.- (a) Fandos, R.; Hernández, C.; Otero, A.; Rodríguez, A.; Ruiz, M. J.; Terrerros, P. *Chem. Eur. J.* **2003**, *9*, 671. (b) Wenzel, B.; Lönnecke, P.; Hey-Hawkins, E. *Organometallics* **2002**, *21*, 2070. (c) Fandos, R.; Otero, A.; Rodríguez, A.; Ruiz, M. J.; Terreros, P. *Angew. Chem. Int. Ed. Engl.* **2001**, *40*, 2884.

6.- (a) Casado, M. A., Pérez-Torrente, J. J.; Ciriano, M. A.; Oro, L. A.; Orejón, A.; Claver, C. *Organometallics* **1999**, *18*, 3035. (b) Atencio, R.; Casado, M. A.; Ciriano, M. A.; Lahoz, F. J.; Pérez-Torrente, J. J.; Tiripicchio, A.; Oro, L. A. *J. Organomet. Chem.* **1996**, *514*, 103.

7.- (a) Casado, M. A.; Pérez-Torrente, J. J.; Ciriano, M. A.; Edwards, A. J.; Lahoz, F. J.; Oro, L. A. *Organometallics* **1999**, *18*, 5299. (b) Casado, M. A.; Pérez-Torrente, J. J.; Ciriano, M. A.; Dobrinovitch, I. T.; Lahoz, F. J.; Oro, L. A. *Inorg. Chem.* **2003**, *42*, 3956.

8.- Casado, M. A.; Ciriano, M. A.; Edwards, A. J.; Lahoz, F. J.; Pérez-Torrente, J. J.; Oro, L. A. *Organometallics* **1998**, *17*, 3414.

9.- Casado, M. A.; Ciriano, M. A.; Edwards, A. J.; Lahoz, F. J.; Oro, L. A.; Pérez-Torrente, J. J. *Organometallics* **1999**, *18*, 3025.

10.- (a) Hernandez-Gruel, M. A. F.; Pérez-Torrente, J. J.; Ciriano, M. A.; Rivas, A. B.; Lahoz, F. J.; Dobrinovitch, I. T.; Oro, L. A. *Organometallics* **2003**, *22*, 1237. (b) Hernandez-Gruel, M. A. F.; Pérez-Torrente, J. J.; Ciriano, M. A.; López, J. A.; Lahoz, F. J.; Oro, L. A. *Eur. J. Inorg. Chem.* **1999**, 2047.

11.- Hernandez-Gruel, M. A. F.; Pérez-Torrente, J. J.; Ciriano, M. A.; Lahoz, F. J.; Oro, L. A. *Angew. Chem. Int. Ed.* **1999**, *38*, 2769.

12.- (a) Kubiak, C. P.; Woodcock, C.; Eisenberg, R. *Inorg. Chem.* **1980**, *19*, 2733. (b) McDonald, R.; Cowie, M. *Inorg. Chem.* **1993**, *32*, 1671.

13.- Lahuerta, P; Latorre, J.; Martínez-Mañez, R.; Payá, J.; Tiripicchio, A.; Tiripicchio-Camellini, M. *Inorg. Chim. Acta* **1993**, *209*, 177.

14.- Antonelli, D. M.; Cowie, M. *Organometallics* **1990**, *9*, 1818.

15.- (a) Freeman, M. A.; Young, D. A. *Inorg. Chem.* **1986**, *25*, 1556. (b) Cowie, M.; Dwight, S. K. *Inorg. Chem.* **1980**, *19*, 2508.

16.- Urazowski, I. F.; Ponomaryov, V. I.; Ellert, O. G.; Nifant'ev, I. E.; Lemenovskii, D. A. *J. Organomet. Chem.* **1988**, *356,* 181.

17.- King, W. A.; Di Bella, S.; Gulino, A.; Lanza, G.; Fragalà, I. L.; Stern, C. L.; Marks, T. *J. Am. Chem Soc.* **1999**, *121*, 355.

18.- Chan, A. S. C.; Shieh, H. –S.; Hill, J. R. *J. Chem. Soc., Chem. Commun.* **1983**, 688.

19.- James. B. R.; Mahajan, D.; Rettig, S. J.; Williams, G. M. *Organometallics* **1983**, *2*, 1452.

20.- (a) Werner, H.; Klingert, B.; Zolk, R.; Rhometzek, P. *J. Organomet. Chem.* **1984**, *266*, 97. (b) Faraone, F.; Bruno, G.; Lo Schiavo, S.; Piraino, P. Bombieri, G. *J. Chem. Soc. Dalton Trans.* **1983**, 1819.

21.- Cotton, F. A. *Prog. Inorg. Chem.* **1976**, *21*, 1.

22.- Haunpt, H. -J.; Flörke, U.; Beckers, H. -G. *Inorg. Chem.* **1994**, *33*, 3481.

23.- Hattori, T.; Matsukawa, S.; Kuwata, S.; Ishii, Y.; Hidai, M. *Chem. Commun.* **2003**, 510.

24.- Heyduk, A. F.; Nocera, D. G. *J. Am. Chem. Soc.* **2000**, *122*, 9415.

25.- Heyduk, A. F.; Macintosh, A. M.; Nocera, D. G. *J. Am. Chem. Soc.* **1999**, *121*, 5023.

26.- Baig, S; Richard, B; Serp, P; Mijoule, C; Hussein, K; Guihery, N; Barthelat, J. C.; Kalck, P. *Inorg. Chem.* **2006**, *45*, 1935.

27.- Hong, F. E.; Chang, Y. C. *B. Chem. Soc. Jpn.* **2004**, *77*, 115.

28.- (a) Schuh, W.; Braunstein, P.; Bénard, M.; Rohmer, M.-M.; Welter, R. Angew. *Chem. Int. Ed.* **2003**, *42*, 2161. (b) Kabashima, S.; Kuwata, S.; Ueno, K.; Shiro, M.; Hidai, M. *Angew. Chem. Int. Ed.* **2000**, *39*, 1128. (c) Venturelli, A.; Rauchfuss, T. B. *J. Am. Chem. Soc.* **1994**, *116*, 4824. (d) Houser, E. J.; Rauchfuss, T. B.; Wilson, S. R. *Inorg. Chem.* **1993**, *32*, 4069.

29.- (a) Tanaka, S.; Bubs, C.; Inagaki, A.; Akita, M. *Organometallics* **2004**, *23*, 317. (b) Akita, M.; Terada, M.; Moro-oka, Y. *Organometallics* **1992**, *11*, 1825.

30.- (a) Carmona, D.; Ferrer, J.; Mendoza, A.; Lahoz, F. J.; Reyes, J.; Oro, L. A. *Angew. Chem. Int. Ed. Engl.* **1991**, *30*, 1171. (b) Bailey, D. A.; Balch, A. L.; Fosset, A.; Olmstead, M. M.; Reedy, P. E., Jr. *Inorg. Chem.* **1987**, *26*, 2413.

31.- [$Cp^{tt}_2Zr(\mu\text{-}S)_2Rh(\mu\text{-}CO)_2(\mu\text{-}dppm)Rh(\eta^2\text{-}dppe)$]. NMR data: $^{31}P\{^{1}H\}$ (CD_2Cl_2, 293 K): δ 47.55 (dd, $J_{Rh\text{-}P}$ = 144 Hz, P_C, dppe), 36.91 (ddt, $J_{Rh\text{-}P}$ = 130 Hz, P_A, dppm), 8.26 (ddtd, $J_{Rh\text{-}P}$ = 135 and 3 Hz, P_B, dppm) (measured $J_{P\text{-}P}$: P_A-P_B = 174 Hz, P_B-P_C = 36 Hz, P_A-P_C = 6 Hz).

32.- (a) Dorta, R; Simón. L.; Milstein, D. *J. Organomet. Chem.* **2004**, *689*, 751. (b) Pettinari, C.; Marchetti, F.; Pettinari, R.; Pizzabiocca, A.; Drozdov, A.; Troyanov, S. I.; Vertlib, V. *J. Organomet. Chem.* **2003**, *688*, 216.

33.- James, B. R.; Mahajan, D. *Can. J. Chem.* **1979**, *57*, 180.

34.- (a) Kubiak, C. P.; Eisenberg, R. *Inorg. Chem.* **1980**, *19*, 2726. (b) Kubiak, C. P.; Eisenberg, R. *Inorg. Chem.* **1980**, *19*, 2726.

35.- SAINT+ Software for CCD difractometers, Bruker AXS, Madison, WI, USA, 2000. Sheldrick, G.M. *SADABS Program for Correction of Area Detector Data*, University of Göttingen, Göttingen, Germany, 1999.

36.- SHELXTL Package v. 6.10, 2000, Bruker AXS, Madison, WI. Sheldrick, G.M. SHELXS-86 and SHELXL-97; University of Göttingen: Göttingen, Germany, 1997.

37.- Gaussian 03, Revision C.02, Frisch, M. J.; Trucks, G. W.; Schlegel, H. B.; Scuseria, G. E.; Robb, M. A.; Cheeseman, J. R.; Montgomery, Jr., J. A.; Vreven, T.; Kudin, K. N.; Burant, J. C.; Millam, J. M.; Iyengar, S. S.; Tomasi, J.; Barone, V.; Mennucci, B.; Cossi, M.; Scalmani, G.; Rega, N.; Petersson, G. A.; Nakatsuji, H.; Hada, M.; Ehara, M.; Toyota, K.; Fukuda, R.; Hasegawa, J.; Ishida, M.; Nakajima, T.; Honda, Y.; Kitao, O.; Nakai, H.; Klene,

M.; Li, X.; Knox, J. E.; Hratchian, H. P.; Cross, J. B.; Bakken, V.; Adamo, C.; Jaramillo, J.; Gomperts, R.; Stratmann, R. E.; Yazyev, O.; Austin, A. J.; Cammi, R.; Pomelli, C.; Ochterski, J. W.; Ayala, P. Y.; Morokuma, K.; Voth, G. A.; Salvador, P.; Dannenberg, J. J.; Zakrzewski, V. G.; Dapprich, S.; Daniels, A. D.; Strain, M. C.; Farkas, O.; Malick, D. K.; Rabuck, A. D.; Raghavachari, K.; Foresman, J. B.; Ortiz, J. V.; Cui, Q.; Baboul, A. G.; Clifford, S.; Cioslowski, J.; Stefanov, B. B.; Liu, G.; Liashenko, A.; Piskorz, P.; Komaromi, I.; Martin, R. L.; Fox, D. J.; Keith, T.; Al-Laham, M. A.; Peng, C. Y.; Nanayakkara, A.; Challacombe, M.; Gill, P. M. W.; Johnson, B.; Chen, W.; Wong, M. W.; Gonzalez, C.; and Pople, J. A.; Gaussian, Inc., Wallingford CT, 2004.

38.- Reed, A.E.; Curtis, L.A.; Weinhold, F. *Chem*. *Rev*. **1988**, *88*, 899.

Table 1. $^{31}P\{^1H\}$ NMR data (C_6D_6) for the compounds $[Cp^{tt}_2Zr(\mu\text{-}S)_2M(\mu\text{-}CO)_2(\mu\text{-}dppm)M'(\eta^2\text{-}dppm)]$ (**3-7**)

	M	M'	δ (ppm)			J (Hz)					
			P_A	P_B	P_C	$Rh\text{-}P_A$	$Rh\text{-}P_B$	$Rh\text{-}P_C$	$P_A\text{-}P_B$	$P_A\text{-}P_C$	$P_B\text{-}P_C$
3	Rh	Rh	42.9 (ddt)	19.8 (ddtd)	-24.5 (ddd)	128	154 / 5	129	175	7	24
4	Ir	Ir	30.6 (dt)	10.6 (dt)	-61.5 (dd)				135	8	45
6	Rh	Ir	46.1 (ddt)	-1.4 (dtd)	-59.9 (ddd)	132	5	4	159	7	40
7	Ir	Rh	26.7 (dt)	31.4 (ddt)	-25.8 (ddd)		160	133	149	8	26

Table 2. Selected Bond Lengths (Å) and Angles (deg) for **3**

_____

|			
Zr-S(1)	2.4329(18)	Zr-S(2)	2.4245(18)
Zr-G(1) [a]	2.314(3)	Zr-G(2) [a]	2.319(3)
Zr-C(Cp^{tt}1) [b]	2.529-2.674(6)	Zr-C(Cp^{tt}2) [b]	2.542-2.678(7)
Rh(1)-S(1)	2.3099(17)	Rh(1)-S(2)	2.4097(18)
Rh(1)-C(27)	2.040(7)	Rh(1)-C(28)	2.062(7)
Rh(1)-P(1)	2.3075(18)	Rh(2)-P(2)	2.3532(19)
Rh(2)-P(3)	2.3313(18)	Rh(2)-P(4)	2.3354(19)
Rh(2)-C(27)	1.993(7)	Rh(2)-C(28)	1.989(7)
C(27)-O(2)	1.154(8)	C(28)-O(1)	1.157(8)
P(1)-C(29)	1.850(6)	P(2)-C(29)	1.823(6)
P(3)-C(54)	1.834(7)	P(4)-C(54)	1.829(7)
S(1)-Zr-S(2)	91.87(6)	G(1)-Zr-G(2) [a]	124.93(11)
S(1)-Zr-G(1) [a]	105.96(9)	S(1)-Zr-G(2) [a]	108.43(9)
S(2)-Zr-G(1) [a]	112.18(9)	S(2)-Zr-G(2) [a]	108.28(9)
P(1)-Rh(1)-S(1)	80.16(6)	P(1)-Rh(1)-S(2)	174.07(6)
P(1)-Rh(1)-C(27)	88.33(19)	P(1)-Rh(1)-C(28)	90.31(18)
S(1)-Rh(1)-C(27)	131.09(19)	S(1)-Rh(1)-C(28)	134.98(19)
S(2)-Rh(1)-C(27)	97.57(19)	S(2)-Rh(1)-C(28)	90.17(18)
S(1)-Rh(1)-S(2)	95.35(6)	C(27)-Rh(1)-C(28)	92.0(3)
P(2)-Rh(2)-P(3)	108.68(7)	P(2)-Rh(2)-P(4)	109.32(7)
P(2)-Rh(2)-C(27)	92.87(19)	P(2)-Rh(2)-C(28)	95.84(19)
P(3)-Rh(2)-C(27)	156.2(2)	P(3)-Rh(2)-C(28)	92.2(2)
P(4)-Rh(2)-C(27)	93.4 (2)	P(4)-Rh(2)-C(28)	152.77(19)

P(3)-Rh(2)-P(4)	70.41(7)	C(27)-Rh(2)-C(28)	95.6(3)
Rh(1)-C(27)-O(2)	129.0(5)	Rh(1)-C(28)-O(1)	129.4(5)
Rh(2)-C(27)-O(2)	144.5(5)	Rh(2)-C(28)-O(1)	144.7(5)
Rh(1)-C(27)-Rh(2)	86.4(3)	Rh(1)-C(28)-Rh(2)	85.9(3)

[a] G(1) and G(2) represent the centroids of the two Cp^{tt} rings. [b] Range values for the Zr-C bond distances of the C(1)-C(5) ($Cp^{tt}1$) and C(14)-C(18) ($Cp^{tt}2$) cyclopentadienyl rings.

Table 3. Crystal Data, Data Collection and Refinement Parameters for the X-Ray Analysis of Complex **3**

formula	$C_{78}H_{86}O_2P_4Rh_2S_2Zr \cdot 2.5\ (C_6H_5CH_3)$
M_r	1770.84
crystal size, mm	0.183 x 0.169 x 0.135
cryst syst	triclinic
space group	*P*-1
a, Å	13.5217(13)
b, Å	14.9233(14)
c, Å	23.258(2)
α, deg	97.010(2)
β, deg	99.872(2)
γ, deg	101.853(2)
Z	2
V, Å^3	4464.5(7)
D_{calc}, g•cm^{-3}	1.317
μ, mm^{-1}	0.644
θ range, deg	1.55-26.00
no. measd rflns	26189
no. unique rflns	17167 (R_{int}= 0.0534)
min / max transm fact	0.891 / 0.928
no rflns /restr/ params	17167 / 26 / 891
$R_1(F)$ ($F^2 \geq 2\ \sigma(F^2)$)	0.0705
$wR_2(F^2)$ (all data)	0.1882
S (all data)	0.993

Caption to the figures
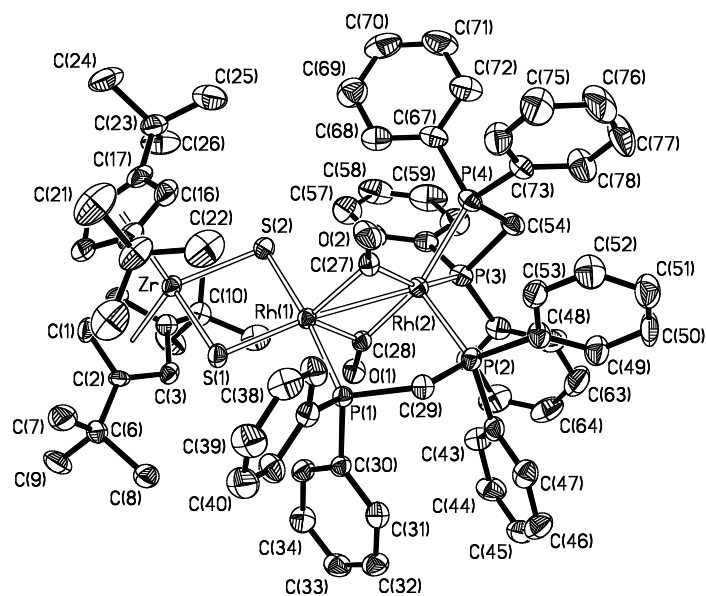
(a)
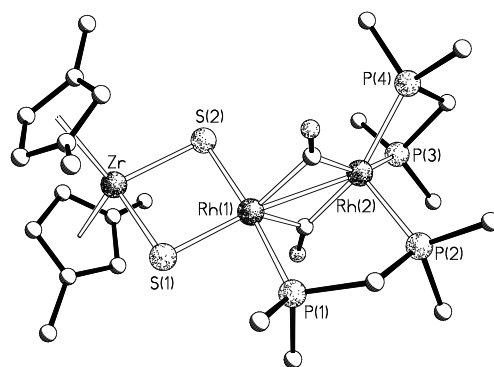
(b)

Figure 1. Molecular diagrams showing the molecular structure of complex [Cp$^{tt}_2$Zr(μ-S)$_2$Rh(μ-CO)$_2$(μ-dppm)Rh(η^2-dppm)] (**3**); (a) ellipsoid representation together with labelling

scheme used; (b) schematic view of the bent trimetallic skeleton (phenyl rings and tert-butyl

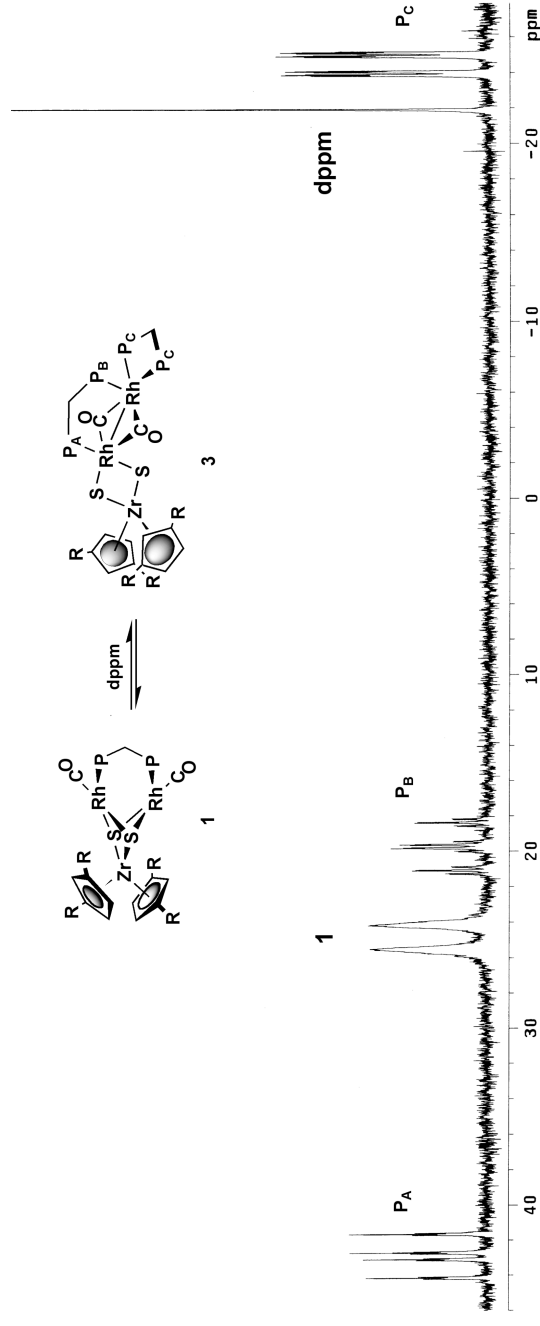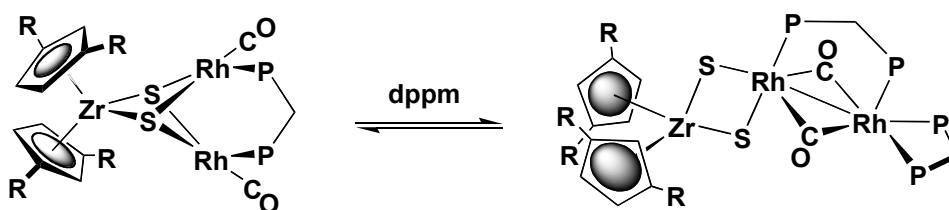substituents are represented by the *ipso* carbon).

Figure 2. $^{31}P\{^1H\}$ NMR spectrum of the equilibrium **1** + dppm $\rightleftarrows$ **3** observed in the reaction of $[Cp^{tt}_2Zr(\mu_3\text{-}S)_2\{Rh(CO)_2\}_2]$ with two molar-equiv of dppm in C_6D_6.

Table of contents and graphical abstract

The dppm-mediated equilibrium between triangular and bent ZrRh$_2$ early-late heterobimetallic compounds (ELHB) involves an intramolecular disproportionation of a Rh(I)···Rh(I) into a metal-metal bonded Rh(II)−Rh(0) dimetal subunits as a consequence of the redistribution of the ligands driven by the incoming dppm ligand.